

Design and Performance Analysis of Multi-scale NOMA for 5G Positioning

Lu Yin, *Member, IEEE*, Jiameng Cao, Zhongliang Deng, Qiang Ni, *Senior Member, IEEE*, Song Li, *Member, IEEE*, Xinyu Zheng, Hanhua Wang

Abstract

This paper presents a feasibility study for a novel positioning-communication integrated signal called Multi-Scale Non-Orthogonal Multiple Access (MS-NOMA) for 5G positioning. One of the main differences between the MS-NOMA and the traditional positioning signal is MS-NOMA supports configurable powers for different positioning users (P-Users) to obtain better ranging accuracy and signal coverage. Our major contributions are: Firstly, we present the MS-NOMA signal and analyze the Bit Error Rate (BER) and ranging accuracy by deriving their simple expressions. The results show the interaction between the communication and positioning signals is rather limited, and it is feasible to use the MS-NOMA signal to achieve high positioning accuracy. Secondly, for an optimal positioning accuracy and signal coverage, we model the power allocation problem for MS-NOMA signal as a convex optimization problem by satisfying the QoS (Quality of Services) requirement and other constraints. Then, we propose a novel Positioning-Communication Joint Power Allocation (PCJPA) algorithm which allocates the powers of all P-Users iteratively. The theoretical and numerical results show our proposed MS-NOMA signal has great improvements of ranging/positioning accuracy than traditional PRS (Positioning Reference Signal) in 5G, and improves the coverage dramatically which means more P-Users could locate their positions without suffering the near-far effect.

Lu Yin, Jiameng Cao, Zhongliang Deng, Xinyu Zheng, and Hanhua Wang are with the School of Electronic Engineering, Beijing University of Posts and Telecommunications, Beijing, 100876, China, e-mail: inlu_mail@bupt.edu.cn, caojiameng@bupt.edu.cn, dengzhl@bupt.edu.cn, buptzxy@bupt.edu.cn, whh0710@bupt.edu.cn.

Qiang Ni is with the School of Computing and Communications, Lancaster University, InfoLab21, LA1 4WA, U.K. e-mail: q.ni@lancaster.ac.uk.

Song Li is with School of Information and Control Engineering, China University of Mining and Technology, Xuzhou, China. e-mail: lisong@cumt.edu.cn.

Index Terms

MS-NOMA, interference, positioning, power allocation.

I. INTRODUCTION

Nowadays, the Location Based Services (LBS) are growing rapidly and attracting much attention with the proliferation of mobile devices [1], [2]. The well known Global Navigation Satellite Systems (GNSS), such as the Global Positioning System (GPS) and the Beidou System (BDS) [3], [4], can only be used in open areas as their signals are easily blocked or interfered by buildings [5]. The emerging Wi-Fi, Bluetooth or Wireless Sensor Networks (WSN) based positioning have well coverage indoors only with dense placements of the nodes [6], [7], [8]. And it is costly for collecting and maintaining the fingerprint database as well [9], [10].

Wireless communication network has a well coverage both indoors and outdoors [11], [12]. Meanwhile, it is cost-effective to be used for positioning purpose as it is ready-made for communication purpose. However, the positioning accuracy can not meet some high-accuracy requirements by using the communication signal directly as the communication system is not designed for positioning purpose specifically [13], [14]. For example, the Positioning Reference Signal (PRS) in the cellular network cannot fully meet the commercial requirements as the discontinuous signal is hardly tracked which leads to a low range measurement accuracy [15]. Moreover, there are severe near-far effects between the positioning signals from different gNBs (next generation NodeBs or called 5G nodeBs) which makes the signals from far gNBs more difficult to be received [16], [17], [18]. Consequently, poor geometric distribution of gNBs is achieved which further worsen the positioning accuracy [19], [20].

To this end, we propose a positioning-communication integrated signal, called Multi-Scale Non-Orthogonal Multiple Access (MS-NOMA), which superposes a low power positioning signal to the communication one without much interference based on the NOMA principle. In time domain, the MS-NOMA signal is Code Division Multiple Access (CDMA) to obtain corresponding spreading gains and ensure a continuous transmission. In frequency domain, Orthogonal Frequency Division Multiplexing Access (OFDMA) is employed for different positioning users as Fig. 1 shows.

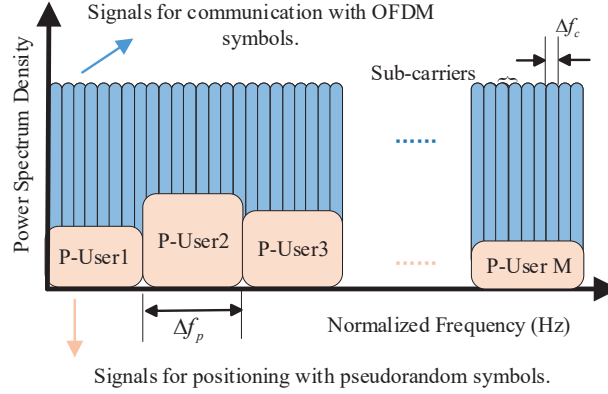


Fig. 1. The MS-NOMA architecture in frequency and power domains

In the proposed MS-NOMA signal, Δf_c and Δf_p represent the sub-carrier spacing of communication user (C-User) and positioning user (P-User), respectively. For the maximum spectrum effectiveness, they are designed as $\Delta f_p = G\Delta f_c$, $G \in \mathbb{N}_+$. We assume both C-User and P-User each occupy a separate sub-carrier, so that there are maximum $N = B/\Delta f_c - 1$ and $M = B/\Delta f_p - 1$ users for communication and positioning purpose, respectively. Where B represents the total bandwidth. The reasons for distinguishing different P-Users are:

- 1) Unlike communication system, it usually needs more than three gNBs to calculate the P-User's position. As the P-Users are located at different locations, the powers of the positioning signals from far gNBs must be high enough in order to be correctly recognized. Meanwhile, the powers of the positioning signals from near gNBs should be low enough to avoid the near-far effect. So different powers for different P-Users are necessary.
- 2) The superposed positioning signal interferes the communication signal like inter-user interference occurred in the normal NOMA as well [21], [22]. To reduce this interference, the power of the positioning signal must be limited under a certain threshold to satisfy the QoS (Quality of Services) requirement of communication. While for P-Users, higher powers are needed for more accurate range measuring [23]. Therefore, the gNBs could transmit positioning signals with different powers for different P-Users to meet the requirements of both C-Users and P-Users.

Although the aforementioned problems may be mitigated by varying the bandwidths of the

positioning signals as well, it will bring some other problems and make the whole system more complicated. In this paper, we discuss the scenario that the bandwidths of all P-Users are identical and fixed. Then, to acquire the highest positioning accuracy over the whole network with the hearability and QoS requirements, the powers of different P-Users must be allocated carefully.

In a conventional OFDM system, it is proved that water-filling over the sub-carriers is the optimal power allocation strategy [24], [25]. However, it does not consider the interferences between different types of users. In [26], where the second user transmit over spectrum holes left in the primary system, an optimal power allocation strategy is proposed. They maximize the down-link capacity of the second user by remaining the interference introduced to the primary user within a tolerable range. In the NOMA system, the power allocation is mostly investigated for signal demodulation and relay transmission [27], [28]. But these algorithms can not be used in our problem that has different models which is more complicated.

To the best of our knowledge, there are few studies about the power allocation in positioning systems which makes our study very challenging. A preliminary part of this study was presented in a letter paper [23]. In this journal version, as compared to [23], we carry out detailed design and conduct more in-depth mathematical performance analysis. The main contributions of this paper are:

- 1) We present the system model of positioning by the proposed MS-NOMA signal and analyze the limitation of positioning by other existing signals.
- 2) We analyze the interferences between the communication and positioning signals of the MS-NOMA signal in the multi-cell scenario. Bit Error Rate (BER) for communication and the ranging error for positioning are derived.
- 3) We model the power allocation problem for the MS-NOMA signal as a convex optimization problem. It minimizes the average positioning error of all P-Users in the network by considering the QoS, the power budget and the hearability requirements. To solve this problem, we propose a novel Positioning-Communication Joint Power Allocation (PCJPA) algorithm which allocates the powers of all P-Users iteratively and derive its solution.
- 4) A series of theoretical and numerical analysis are done to evaluate the feasibility of positioning by MS-NOMA signal. The results show our proposed MS-NOMA signal has

a great improvement of ranging accuracy than PRS in traditional 5G signal, and improves the coverage dramatically which means more P-Users could locate their positions without suffering the near-far effect.

Notations: $\|\cdot\|$ represents the Euclidean distance. The operator $\text{cov}(\cdot)$ represents the covariance. kn and km represent the n^{th} C-User/communication signal and the m^{th} P-User/positioning signal served/broadcast by gNB k , respectively. \mathcal{M} , \mathcal{N} , \mathcal{K} and \mathcal{K}^k represent the set $\{1, \dots, M\}$, $\{1, \dots, N\}$, $\{1, \dots, K\}$ and $\{1, \dots, k-1, k+1, \dots, K\}$, respectively.

II. SYSTEM MODEL

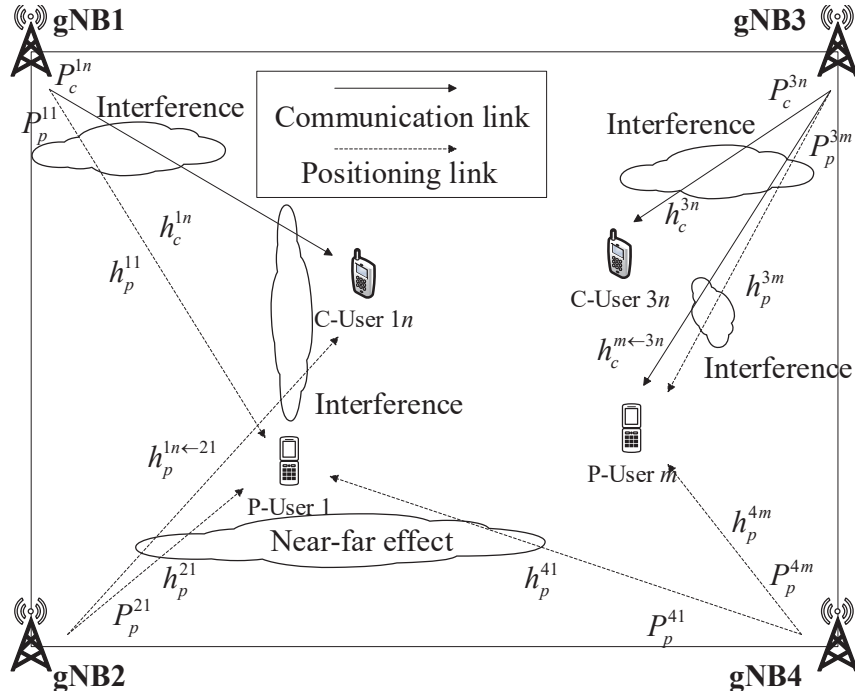


Fig. 2. System model of positioning by the MS-NOMA signal

Consider a typical positioning scenario in spatial domain with K gNBs as Fig. 2 shows. C-Users and P-Users may be located at different locations. Because each C-User connects only one gNB, there are maximum KN C-Users in the network. While a P-User needs as many connections as possible for accurate positioning. So, there are maximum M P-Users in the network under the assumption that all gNBs server the same P-Users.

To ensure the P-Users receiving more than one gNB's signal, the powers of the positioning signals should be strong enough. Then, this strong positioning signal may interfere the neighbor C-Users. To examine these interferences, let us define h_c^{kn} and h_p^{km} as the instantaneous channel gains between gNB k and C-User kn /P-User m , respectively. Notice that the communication/positioning signal broadcast from gNB k' to the C-User $k'n$ /P-User m will be received by the P-User m /C-User kn as well, we use $h_c^{m\leftarrow k'n}$ and $h_p^{kn\leftarrow k'm}$ to represent these two instantaneous channel gains, respectively.

Without any loss of generality, we assume: 1) Each spreading sequence for different P-Users is independent; 2) The powers for all C-Users are identical and the powers for all P-Users are to be allocated; and 3) The channel states are available through a delay- and error-free feedback channel which are known by the gNBs.

What we concern is the horizontal positioning accuracy¹. If the gNBs are perfectly synchronized, the P-Users will use time-based algorithm to fix their locations. Then, the horizontal positioning accuracy of P-User m can be expressed as

$$\Psi^m = \sqrt{\sum_{k \in \mathcal{K}} (\lambda^{km} \sigma_\rho^{km})^2} \quad (1)$$

where λ^{km} and σ_ρ^{km} are given in Appendix A.

III. FEATURES OF MS-NOMA SIGNAL

A. Interference of the Positioning Signal to Communication One

For evaluating the interference of the positioning signal to communication one, we assume the inter-cell interference between the communication signals could be ideally eliminated. Then, the BER of C-User kn is [30]

$$BER^{kn} = \text{Erfc} \left(\frac{\gamma |h_c^{kn}|^2 P_c T_c}{I^{kn} + 2N_0} \right) \quad (2)$$

¹The vertical positioning accuracy of terrestrial system is usually very larger as the large vertical dilution [29]. Other methods are usually used to estimate vertical position rather than terrestrial positioning system [6], [17].

where Γ and γ are determined by the modulation and coding schemes. P_c is the power of the communication signal. T_c is the period of the communication symbol. N_0 is the environment noise's single-sided Power Spectral Density (PSD). I^{kn} represents the interference of the positioning signal to the C-User kn . Notice that the powers of the positioning signals from different gNBs may be similar by power allocation, the interferences caused by the positioning signals from the neighbor gNBs can not be ignored. Then we have

$$I^{kn} = \sum_{k' \in \mathcal{K}} \sum_{m \in \mathcal{M}} \bar{P}_p^{kn \leftarrow k'm} \quad (3)$$

where $\bar{P}_p^{kn \leftarrow k'm}$ is the power of the positioning signal $k'm$ received by C-User kn which satisfies

$$\begin{aligned} \bar{P}_p^{kn \leftarrow k'm} &= \left| h_p^{kn \leftarrow k'm} \right|^2 P_p^{k'm} G_p^m(n\Delta f_c) \\ &= \left| h_p^{kn \leftarrow k'm} \right|^2 P_p^{k'm} T_p \text{sinc}^2 \left(m - \frac{n}{G} \right) \end{aligned} \quad (4)$$

where $P_p^{k'm}$ is the power of positioning signal m broadcast by gNB k' . $G_p^m(f)$ is the normalized PSD of positioning signal m which satisfies

$$G_p^m(f) = T_p \text{sinc}^2 [(f - m\Delta f_p) T_p] \quad (5)$$

where T_p is the period of the positioning symbol.

B. Ranging Accuracy of MS-NOMA Signal

The receiver could use a Delay Locked Loop (DLL) to track the positioning signal. Taking the coherent early-late discriminator for example [31], the tracking/ranging error of the positioning signal km can be written as

$$\begin{aligned} (\sigma_p^{km})^2 &= \\ & \frac{a \int_{B_0 - B_{fe}/2}^{B_0 + B_{fe}/2} [N_0 + G_s^m(f + m\Delta f_p) + G_q^{km}(f + m\Delta f_p)] G_p^m(f + m\Delta f_p) \sin^2(\pi f D T_p) df}{\left| h_p^{km} \right|^2 P_p^{km} \left[2\pi \int_{B_0 - B_{fe}/2}^{B_0 + B_{fe}/2} f G_p^m(f + m\Delta f_p) \sin(\pi f D T_p) df \right]^2} \end{aligned} \quad (6)$$

where a is determined by the loop parameters. B_0 is the central frequency of MS-NOMA signal. B_{fe} is the double-sided front-end bandwidth. D is the early-late spacing of DLL. $G_s^m(f)$ is the PSD of the communication signals received by P-User m which satisfies

$$G_s^m(f) = \sum_{k' \in \mathcal{K}} \sum_{n \in \mathcal{N}} \left| h_c^{m \leftarrow k' n} \right|^2 P_c G_c^n(f) \quad (7)$$

where $G_c^n(f) = T_c \text{sinc}^2[(f - n\Delta f_c) T_c]$ is the normalized PSD of communication signal n . $G_q^{km}(f)$ is the PSD of the positioning signals from other gNBs which satisfies

$$G_q^{km}(f) = \sum_{k' \in \mathcal{K}^k} \left| h_p^{k' m} \right|^2 P_p^{k' m} G_p^m(f) \quad (8)$$

By taking (5), (7)-(8) into (6) and using some approximations, (6) can be simplified to

$$(\sigma_\rho^{km})^2 \approx \frac{aT_p^2}{2} \left[\frac{1}{B_{fe} T_p (C/N_0)^{km}} + \frac{B \sum_{k' \in \mathcal{K}} (CPR)^{km \leftarrow k'}}{2B_{fe}^2} + \frac{\sum_{k' \in \mathcal{K}^k} (PPR)^{km \leftarrow k' m}}{B_{fe}^2 T_p} \right] \quad (9)$$

where $(C/N_0)^{km}$, $(CPR)^{km \leftarrow k'}$ and $(PPR)^{km \leftarrow k' m}$ can be found in Appendix B. The first item in (9) is caused by the noise, the second one is caused by the communication signals from all gNBs, and the third one is caused by the other gNBs' positioning signals.

We define the ranging-factor $(\tilde{\sigma}_\rho^{km})^2 = (\sigma_\rho^{km})^2 P_p^{km}$ as (10) shows for later use.

$$(\tilde{\sigma}_\rho^{km})^2 = \frac{aT_p^2}{2} \left[\frac{N_0}{B_{fe} T_p |h_p^{km}|^2} + \frac{BGP_c \sum_{k' \in \mathcal{K}} |h_c^{m \leftarrow k'}|^2}{B_{fe}^2 |h_p^{km}|^2} + \frac{\sum_{k' \in \mathcal{K}^k} |h_p^{k' m}|^2 P_p^{k' m}}{B_{fe}^2 T_p |h_p^{km}|^2} \right] \quad (10)$$

IV. THE POWER ALLOCATION OF MS-NOMA SIGNAL

A. The Constraints

1) *The BER Threshold under QoS Constraint:* To ensure the QoS of the C-Users, the BER of all C-Users should be limited under a certain threshold

$$BER^{kn} \leq \Xi_{th}, \quad \forall k \in \mathcal{K}, \forall n \in \mathcal{N} \quad (11)$$

Then, by taking (2) to (11) and rearranging items, we have

$$I^{kn} \leq \frac{\gamma |h_c^{kn}|^2 P_c T_c}{\text{erfc}^{-1}(\Xi_{th}/\Gamma)} - 2N_0$$

$$\triangleq I_{th}^{kn}, \quad \forall k \in \mathcal{K}, \forall n \in \mathcal{N} \quad (12)$$

where I_{th}^{kn} is defined as the interference threshold of C-User kn which is determined by the QoS requirement Ξ_{th} .

2) *The Total Power Limitation:* The total transmit power is often limited. In MS-NOMA signal, we have

$$\sum_{m \in \mathcal{M}} P_p^{km} + NP_c \leq P_T^k, \quad \forall k \in \mathcal{K} \quad (13)$$

where P_T^k is the total transmit power of gNB k . Let's define the positioning power budget of gNB k as $P_{th}^k = P_T^k - NP_c$, then we have

$$\sum_{m \in \mathcal{M}} P_p^{km} \leq P_{th}^k, \quad \forall k \in \mathcal{K} \quad (14)$$

3) *The Elimination of Near-far Effect:* To guarantee P-Users receive as many positioning signals as possible, the powers of the received positioning signals from different gNBs must satisfy

$$\frac{|h_p^{km}|^2 P_p^{km}}{|h_p^{k'm}|^2 P_p^{k'm}} \geq \varrho \Omega, \quad \forall m \in \mathcal{M}, \forall k \in \mathcal{K}, \forall k' \in \mathcal{K}^k \quad (15)$$

where Ω is the positioning signal's auto-correlation to cross-correlation ratio which is determined by the pseudorandom code and its length. ϱ is determined by the receiver's performance which is usually larger than 1. For a particular positioning signal km , if the strongest cross-correlation satisfies (15), all k' s in (15) will be satisfied. So (15) can be rewritten as

$$|h_p^{km}|^2 P_p^{km} \geq \varrho \Omega |h_p^{k'_k m}|^2 P_p^{k'_k m}, \quad \forall m \in \mathcal{M}, \forall k \in \mathcal{K} \quad (16)$$

where $k'_k m$ represents the index of the strongest signal received by the P-User km except the positioning signal km .

B. The Proposed Joint Power Allocation Model

Our goal is to obtain a best positioning performance for all P-Users in terms of both coverage and accuracy under QoS requirement and total transmit power budget. So, the average horizontal positioning accuracy² for all P-Users in the network is minimized by finding the power values $P_p^{km}, \forall m \in \mathcal{M}, \forall k \in \mathcal{K}$ under the given constraints. We use the fact that maximization of negative value of a convex function is equivalent to its minimization. Mathematically, the power allocation problem can be formulated as a convex optimization problem as follows

$$\text{OP1} : \max_{P_p^{km}} - \frac{1}{M} \sum_{m \in \mathcal{M}} (\Psi^m)^2 \quad (17)$$

$$\text{s.t. } I^{kn} \leq I_{th}^{kn}, \quad \forall n \in \mathcal{N}, \forall k \in \mathcal{K} \quad (18)$$

$$\sum_{m \in \mathcal{M}} P_p^{km} \leq P_{th}^k, \quad \forall k \in \mathcal{K} \quad (19)$$

$$|h_p^{km}|^2 P_p^{km} \geq \varrho \Omega |h_p^{k'm}|^2 P_p^{k'm}, \quad \forall m \in \mathcal{M}, \forall k \in \mathcal{K} \quad (20)$$

OP1 can be solved by the Lagrange duality method [32]. Then the Lagrangian of OP1 can be written as

$$\begin{aligned} \mathcal{L}(\{P_p^{km}\}, \mu, \nu, \beta) = & -\frac{1}{M} \sum_{m \in \mathcal{M}} \sum_{k \in \mathcal{K}} (\lambda^{km} \sigma_p^{km})^2 + \sum_{k \in \mathcal{K}} \sum_{n \in \mathcal{N}} \mu^{kn} (I_{th}^{kn} - I^{kn}) \\ & + \sum_{k \in \mathcal{K}} \nu^k \left(P_{th}^k - \sum_{m \in \mathcal{M}} P_p^{km} \right) + \sum_{m \in \mathcal{M}} \sum_{k \in \mathcal{K}} \beta^{km} \left(|h_p^{km}|^2 P_p^{km} - \varrho \Omega |h_p^{k'm}|^2 P_p^{k'm} \right) \end{aligned} \quad (21)$$

where μ , ν and β are the matrices of dual variables associated with the corresponding constraints given in (12), (14) and (15)

$$\mu = \{\mu^{kn}, \forall k \in \mathcal{K}, \forall n \in \mathcal{N}\} \in \mathbb{C}^{K \times N} \succeq 0 \quad (22)$$

$$\nu = \{\nu^k, \forall k \in \mathcal{K}\} \in \mathbb{C}^{1 \times K} \succeq 0 \quad (23)$$

$$\beta = \{\beta^{km}, \forall k \in \mathcal{K}, \forall m \in \mathcal{M}\} \in \mathbb{C}^{K \times M} \succeq 0 \quad (24)$$

²For calculation convenience, we use the square of the horizontal positioning accuracy, i.e. $(\Psi^m)^2$

The Lagrange dual function of OP1 is then given by

$$g(\mu, \nu, \beta) = \max_{P_p^{km}} \mathcal{L}(\{P_p^{km}\}, \mu, \nu, \beta) \quad (25)$$

The dual optimization problem can be formulated as

$$\text{ming}(\mu, \nu, \beta) \quad (26)$$

$$\text{s.t. } \mu \succeq 0, \nu \succeq 0, \beta \succeq 0 \quad (27)$$

Obviously, $\mathcal{L}(\{P_p^{km}\}, \mu, \nu, \beta)$ is linear in μ, ν, β for fixed P_p^{km} , and $g(\mu, \nu, \beta)$ is the maximum of linear functions. Thus, the dual optimization problem is always convex. In the following, the dual decomposition method introduced in [33] is employed to solve this problem. For this purpose, we introduce a transformation $\sum_{n \in \mathcal{N}} = \sum_{m \in \mathcal{M}} \sum_{n \in \mathbb{N}_m}$ to decompose the Lagrange dual function to $K \times M$ independent sub-problems, where

$$\mathbb{N}_m = \{(2G - 1)(m - 1) + 1, \dots, (2G - 1)m\} \quad (28)$$

Then we have

$$g(\mu, \nu, \beta) = \sum_{k \in \mathcal{K}} [g^k(\mu, \nu, \beta)] \quad (29)$$

$$= \sum_{k \in \mathcal{K}} \left\{ \sum_{m \in \mathcal{M}} g^{km}(\mu, \nu, \beta) + \nu^k P_{th}^k \right\} \quad (30)$$

where

$$g^{km}(\mu, \nu, \beta) = \max_{P_p^{km}} \left\{ -\frac{1}{M} (\lambda^{km} \sigma_\rho^{km})^2 - \nu^k P_p^{km} + \sum_{n \in \mathbb{N}_m} \mu^{kn} (I_{th}^{kn} - I^{kn}) \right. \\ \left. + \beta^{km} (|h_p^{km}|^2 P_p^{km} - \varrho \Omega |h_p^{k'm}|^2 P_p^{k'm}) \right\} \quad (31)$$

From (31), it is clear that we can decompose the Lagrange dual function $g^k(\mu, \nu, \beta)$ to M

independent sub-problems by giving ν^k . Each of the sub-problems is given by

$$\text{OP2} : \max_{P_p^{km}} -\frac{1}{M} (\lambda^{km} \sigma_\rho^{km})^2 - \nu^k P_p^{km} \quad (32)$$

$$\text{s.t. } I^{kn} \leq I_{th}^{kn}, \quad n \in \mathbb{N}_m \quad (33)$$

$$|h_p^{km}|^2 P_p^{km} \geq \varrho \Omega |h_p^{k'm}|^2 P_p^{k'm} \quad (34)$$

The Lagrangian of OP2 is

$$\begin{aligned} \tilde{\mathcal{L}} \left(\{P_p^{km}\}, \tilde{\mu}^{kn}, \tilde{\beta}^{km} \right) &= -\frac{1}{M} (\lambda^{km} \sigma_\rho^{km})^2 - \nu^k P_p^{km} + \sum_{n \in \mathbb{N}_m} \tilde{\mu}^{kn} (I_{th}^{kn} - I^{kn}) \\ &+ \tilde{\beta}^{km} \left(|h_p^{km}|^2 P_p^{km} - \varrho \Omega |h_p^{k'm}|^2 P_p^{k'm} \right) \end{aligned} \quad (35)$$

where $\tilde{\mu}^{kn}$ and $\tilde{\beta}^{km}$ are the non-negative dual variables for constraints (33) and (34), respectively.

The Lagrange dual function of OP2 is given by

$$\tilde{g}^{km} \left(\tilde{\mu}^{kn}, \tilde{\beta}^{km} \right) = \max_{P_p^{km}} \tilde{\mathcal{L}} \left(\{P_p^{km}\}, \tilde{\mu}^{kn}, \tilde{\beta}^{km} \right) \quad (36)$$

The dual problem is then expressed as

$$\min \tilde{g}^{km} \left(\tilde{\mu}^{kn}, \tilde{\beta}^{km} \right) \quad (37)$$

$$\text{s.t. } \tilde{\mu}^{kn} \geq 0, \quad \forall n \in \mathbb{N}_m \quad (38)$$

$$\tilde{\beta}^{km} \geq 0 \quad (39)$$

The optimal power allocation solution \tilde{P}_p^{km} of OP2 can be obtained by using the Karush-Kuhn-Tucker (KKT) conditions as (40) shows.

$$\tilde{P}_p^{km} = \underbrace{\lambda^{km}}_{\text{geometric-dilution}} \times \underbrace{\tilde{\sigma}_\rho^{km}}_{\text{ranging-factor}} \times \underbrace{\left[M \left(\tilde{\beta}^{km} |h_p^{km}|^2 - \nu^k - \sum_{n \in \mathbb{N}_m} \tilde{\mu}^{kn} J^{kn \leftarrow m} \right) \right]^{-1/2}}_{\text{constraint-scale}} \quad (40)$$

where $J^{kn \leftarrow m}$ can be found in Appendix C.

C. Remarks

From (40), it is observed that the optimal power allocation solution is determined by the geometric-dilution, ranging-factor and constraint-scale. It is necessary to have a clear understanding of these factors that affect the allocated power.

The geometric-dilution λ^{km} associates with the relative positions between the P-User and all gNBs. This means the power allocation procedure does not only minimize the ranging accuracy, but also considers the geometric distribution which affects the positioning accuracy as well.

The ranging-factor $\tilde{\sigma}_\rho^{km}$ reflects the ranging ability of P-User as (10) shows. If the loop parameters are fixed, $\tilde{\sigma}_\rho^{km}$ is determined by the channel gains of a certain P-User m , i.e. $|h_p^{km}|^2$, $|h_c^{m \leftarrow k'}|^2$ and $|h_p^{k'm}|^2$ which reflect the attenuation of the positioning signal, the communication signals and the other positioning signals, respectively. If the positioning signal's attenuation is large, i.e. $|h_p^{km}|^2$ is small, it will allocate a stronger positioning power, and vice versa. Conversely, if the communication signals' attenuation is large, i.e. $|h_c^{m \leftarrow k'}|^2$ is small, it will allocate a weak positioning power because of the small interference from the communication signals, and vice versa. Please notice that $\sum_{k' \in \mathcal{K}} |h_c^{m \leftarrow k'}|^2$ in $\tilde{\sigma}_\rho^{km}$ will converge to $|h_c^{m \leftarrow k}|^2$ if the communication signals from all other gNBs (except gNB k) are weak enough. However, different from $|h_p^{km}|^2$ and $|h_c^{m \leftarrow k'}|^2$, there is no monotonic relation between the allocated power and $|h_p^{k'm}|^2$ as $|h_p^{k'm}|^2$ will be weighted by the powers of the positioning signals broadcast by the other gNBs, i.e. $P_p^{k'm}$ s.

The constraint-scale reflects the impact of the constraints:

$\tilde{\mu}^{kn}$ is the dual variable associated with the BER threshold of C-User kn . If C-User kn can accommodate a higher BER, $\tilde{\mu}^{kn}$ will be smaller, and thus result in a higher constraint-scale, and vice versa. In the extreme case that C-User kn cannot accommodate any additional interference, $\tilde{\mu}^{kn}$ will be infinity, and thus the constraint-scale will be zero, which indicates that the positioning signal over C-User kn 's band is not permitted. On the contrary, if C-User kn has no requirement on the BER, $\tilde{\mu}^{kn}$ will be zero, and thus the power-scale will be only determined by the other constraints.

$J^{kn \leftarrow m}$ is determined by the channel gains of positioning signals $k'm$ ($k' \in \mathcal{K}$) at C-User kn as (67) shows. It is clear that a smaller $\sum_{k' \in \mathcal{K}} |h_p^{kn \leftarrow k'm}|^2$ will result in a higher constraint-scale. This

is intuitively correct because the P-Users' transmissions from all gNBs will not cause too much interference when $\sum_{k' \in \mathcal{K}} |h_p^{kn \leftarrow k'm}|^2$ is small. In the real scenarios, if $\sum_{k' \in \mathcal{K}} |h_p^{kn \leftarrow k'm}|^2 \rightarrow 0$, which means C-User kn is too far from all gNBs to receive any communication/positioning signal, the P-Users will not cause any interferences to this C-User no matter how strong its transmit power is. If C-User kn is far from all gNBs except its own cell, i.e. $\sum_{k' \in \mathcal{K}} |h_p^{kn \leftarrow k'm}|^2 \rightarrow h_p^{kn \leftarrow km} \approx h_c^{kn}$, the positioning signals from other gNBs will not interference the C-Users.

ν^k is the dual variable associated with the transmit power budget. A larger power budget results in a smaller ν^k , and thus results in a lower ranging error, and vice versa.

$\tilde{\beta}^{km}$ is a parameter related to the P-User's receiver performance. It reflects the influence of the cross-correlation (i.e. (15)) on the constraint-scale. There will be a higher $\tilde{\beta}^{km}$ with a smaller ρ . Namely, if the receiver has a better anti-cross-correlation performance, there will be a higher ranging accuracy and better coverage, vice versa.

D. The Positioning-Communication Joint Power Allocation Scheme

The remaining task for solving OP1 is to obtain the optimal dual variables, which are the same in both OP1 and OP2. Applying the solution to OP2, we can obtain the optimal power allocation \tilde{P}_p^{km} in OP1. However, it is difficult to solve OP2 directly because we cannot obtain the closed-form expression for dual variables. The Lagrange dual function (29) is made up of K independent sub-problems. For each sub-problem, it is observed that ν^k is the same for all P-Users. μ^{kn} and β^{km} are different for C-Users and P-Users, respectively. Then, we can solve the optimization problem using hierarchical algorithm by updating the values of the dual variables $\{\mu, \nu, \beta\}$ via subgradient methods, which guarantees the gradient-type algorithm to converge to the optimal solution [34].

Proposition: The subgradients of $\tilde{g}^{km}(\tilde{\mu}^{kn}, \tilde{\beta}^{km})$ are given by $\dot{\mu}^{kn} = I_{th}^{kn} - I^{kn}$ and $\dot{\beta}^{km} = |h_p^{km}|^2 P_p^{km} - \rho \Omega |h_p^{k'm}|^2 P_p^{k'm}$. Then, \tilde{P}_p^{km} is the optimal solution obtained at $\tilde{\mu}^{kn}$ and $\tilde{\beta}^{km}$. Next, ν^k is updated by its subgradient, which is given by $\dot{\nu}^k = P_{th}^k - \sum_{m \in \mathcal{M}} P_p^{km}$. Finally, $\hat{P}_p = \left\{ \tilde{P}_p^{km}, \forall k \in \mathcal{K}, \forall m \in \mathcal{M} \right\}$ is the optimal solution obtained at ν^k under the given μ^{kn} and β^{km} .

Proof: Please see the Appendix D.

Using the above gradient, we can obtain the optimal power allocation by iterative Lagrangian multiplier $\{\mu, \nu, \beta\}$. Notice that the positions and powers of P-Users are unknown which are necessary for calculating the geometric-dilution λ^{km} and the ranging factor $\tilde{\sigma}_\rho^{km}$, respectively. We can minimize the ranging error for all positioning users without considering the impact of the geometric-dilution and the impact of multiple access at the first iteration. Then, we can get approximate positions and initial allocated powers. After several iterations, the positions and the powers will be converge to the optimal values.

The algorithm to solve OP1 can be summarized as Algorithm 1 shows. Where t and t' are the iteration numbers. $iterN$ is the maximum iteration amount. b_1 , b_2 and b_3 are the update step sizes. $\varepsilon > 0$ is a given small constant.

Algorithm 1 The proposed PCJPA algorithm

- 1: Initial the dual variable ν_1^k for all $k \in \mathcal{K}$ **in parallel**
 - 2: **for** $t = 1$ to $iterN$ **do**
 - 3: Initial $\mu_1^{kn}, \beta_1^{km}, P_p^{k'm}$ for all $n \in \mathcal{N}$, $m \in \mathcal{M}$ and $k' \in \mathcal{K}^k$ **in parallel**
 - 4: **for** $t' = 1$ to $iterN$ **do**
 - 5: For each P-User m , calculate \tilde{P}_p^{km} using (40)
 - 6: Update $\mu_{t'}^{kn}$ and $\beta_{t'}^{km}$ by their subgradient:
 - 7: i) $\tilde{\mu}_{t'+1}^{kn} = \mu_{t'}^{kn} - b_2 \dot{\mu}^{kn}$
 - 8: ii) $\tilde{\beta}_{t'+1}^{km} = \beta_{t'}^{km} - b_3 \dot{\beta}^{km}$
 - 9: Update $P_p^{km} = \tilde{P}_p^{km}$ for all $k \in \mathcal{K}$ and $m \in \mathcal{M}$
 - 10: **if** $|\tilde{\mu}_{t'+1}^{kn} - \mu_{t'}^{kn}| \leq \varepsilon$ & $|\tilde{\beta}_{t'+1}^{km} - \beta_{t'}^{km}| \leq \varepsilon$ **then**
 - 11: break
 - 12: **end if**
 - 13: **end for**
 - 14: Update ν_{t+1}^k by its subgradient:
 - 15: $\tilde{\nu}_{t+1}^k = \nu_t^k - b_1 \dot{\nu}^k$
 - 16: **if** $|\tilde{\nu}_{t+1}^k - \nu_t^k| \leq \varepsilon$ **then**
 - 17: break
 - 18: **end if**
 - 19: **return** $\hat{P}_p = \left\{ \tilde{P}_p^{km}, \forall k \in \mathcal{K}, \forall m \in \mathcal{M} \right\}$
-

V. THE PERFORMANCE EVALUATION

In this section, we evaluate the communication and ranging performances of the proposed MS-NOMA signal under a single cell network firstly. Then, we examine the positioning performance

in a 4-gNBs cell by considering the impact of all factors comprehensively. In the single cell scenario, the impact of the cross-correlation will be vanished and the channel gains of the communication and positioning signals will be seen as equal. Then, (2) and (9) become

$$BER^n = \Gamma \operatorname{erfc} \left(\frac{\gamma P_c T_c}{I^n + 2N_0} \right) \quad (41)$$

$$(\sigma_\rho^m)^2 \approx \frac{aT_p^2}{2} \left[\frac{1}{B_{fe} T_p (C/N_0)^m} + \frac{B (CPR)^m}{2B_{fe}^2} \right] \quad (42)$$

where

$$I^n = \sum_{m=1}^M P_p^m T_p \operatorname{sinc}^2 \left(m - \frac{n}{G} \right) \quad (43)$$

$$(C/N_0)^m = P_p^m / N_0 \quad (44)$$

$$(CPR)^m = 2GP_c / P_p^m \quad (45)$$

Notice that (41) and (42) reflect the features of MS-NOMA signal itself without interferences from other gNBs.

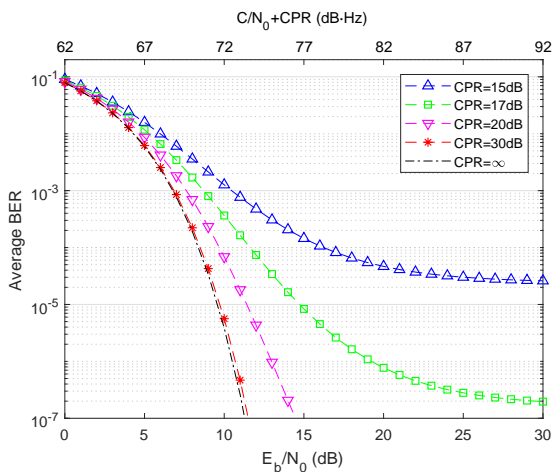
The simulation settings are: The communication and positioning signals use QPSK and BPSK constellation, respectively. The carrier frequency is set to 3.5GHz and $\Delta f_c = 30\text{kHz}$. Two scenarios with different bandwidths of positioning signals are considered: 1) $B = 20\text{MHz}$ 2) $B = 50\text{MHz}$. The amount of P-User is $M = 20$, i.e. the positioning signal is 30/80 times faster than the communication one under 20/50MHz bandwidth, respectively. The powers of all C-Users are assumed as identical. The front-end bandwidth is set to twice of the total bandwidth, i.e. $B_{fe} = 2B$. The loop parameters are set as: $B_L = 0.2\text{Hz}$, $T_{coh} = 0.02\text{s}$ and $D = 0.02\text{chips}$, where B_L is the code loop noise bandwidth and T_{coh} is the predetection integration time.

A. Communication Performance

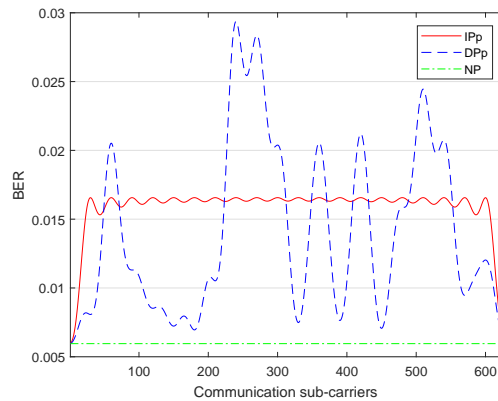
We firstly examine the interference of the positioning signal to the C-Users. Fig. 3a shows the average BERs over the whole bandwidth when $P_p^m = P_p, \forall m \in \mathcal{M}$. It is clear that the

average BERs decrease with the increasing of E_b/N_0 as well as C/N_0 ($E_b = P_c T_c$ is the energy of the communication symbol). Notice that the BER curves with small CPR will tend to be flat when E_b/N_0 becomes larger. This is because the interference caused by the positioning signal dominates the BER performance rather than the environment noise (i.e. I^n is much larger than $2N_0$). When the positioning signal becomes weaker (CPR becomes larger), the BER curves will become flat with larger E_b/N_0 and they will become closer to the one that only exists noise (CPR = ∞).

Fig. 3b detailed shows the BERs for each C-User. If the powers of the P-Users are identical (IPp), the BERs are approximately identical as well. While the BERs are different when the P-Users' powers are different (DPP). Then, the maximum BER is related to all P-Users' powers (see (41)) in this case. Of course, both of the IPp and DPP are higher than the scenario that do not exist positioning signals (NP).



(a) Average BER in different scenarios



(b) BER of the communication signal. $E_b/N_0 = 5\text{dB}$, $CPR = 15\text{dB}$

Fig. 3. Communication Performance

B. Ranging Performance

We then examine the range measurement accuracy of the MS-NOMA signal. The ranging accuracy of the MS-NOMA and PRS signal are compared. Where the lower bound of PRS is used as introduced in [35].

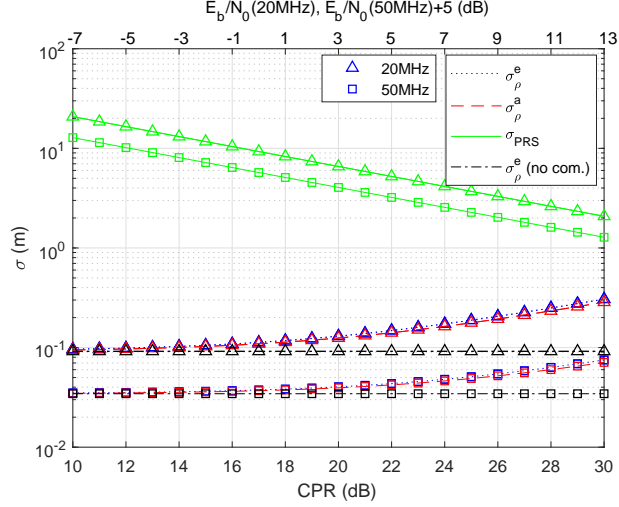


Fig. 4. Range measurement accuracy at $C/N_0 = 45\text{dB} \cdot \text{Hz}$

Fig. 4 shows the range measurement accuracy when $C/N_0 = 45\text{dB} \cdot \text{Hz}$. Where superscript e and a represent the exact and approximate results, respectively. It is clear that the measurement errors of the MS-NOMA signal are always smaller than the ones of the PRS signal when $\text{CPR} < 30\text{dB}$. And the ranging accuracy of the 20MHz MS-NOMA signal is even much higher than the one of the 50MHz PRS signal. The accuracy gap between the two signals becomes larger when CPR decreases. It is because when the power of the communication signal decreases, its interference to the positioning one becomes weaker. While the measurement accuracy of PRS becomes worse due to the lower signal-to-noise ratio of the communication signal.

Please notice that the curves of the MS-NOMA signal will not change if the communication power is fixed and the positioning one is variable. For example, if $E_b/N_0 = 0\text{dB}$ and C/N_0 varies from 32 to 52dB·Hz (i.e. $10\text{dB} < \text{CPR} < 30\text{dB}$) with 20MHz bandwidth, the measurement accuracy of PRS is fixed at 9.29m and the accuracy of MS-NOMA is the same as Fig. 4 shows. Then, the measurement error will decrease when the power of the positioning signal increases.

Although stronger positioning power will have higher measurement accuracy, the maximum power of the positioning signals will be limited by the QoS of communication as Fig. 3 shows. So, P_p^m s must be allocated carefully to acquire the best ranging performance under the QoS

constraint. In the real application, both of the communication and positioning interferences from other gNBs, must be considered which will be evaluated next subsection.

Fig. 4 also confirms that the approximations of σ_ρ (see (42)) correspond to the exact one (see (6)) very well. And all of them are decimeter or centimeter level which ensures sub-meter level positioning accuracy compare to the meter level positioning accuracy of PRS. Meanwhile, the measurement error is only a little larger than the one that without communication signal, which means the effect of the communication signal is limit to the range measuring.

C. Positioning Performance

In this section, we present the numerical results to evaluate the positioning performance of MS-NOMA signal by using the proposed PCJPA algorithm. The gNBs are fixed at $(0, 0)$, $(0, 200)$, $(200, 200)$, $(200, 0)$ and 20 P-Users are randomly distributed in the coverage area. The free space propagation model is employed with 50 Monte Carlo runs in each simulation. Without any loss of generality, we set $P_{th}^k = P_{th}$ for any $k \in \mathcal{K}$ and $\varrho = 2$.

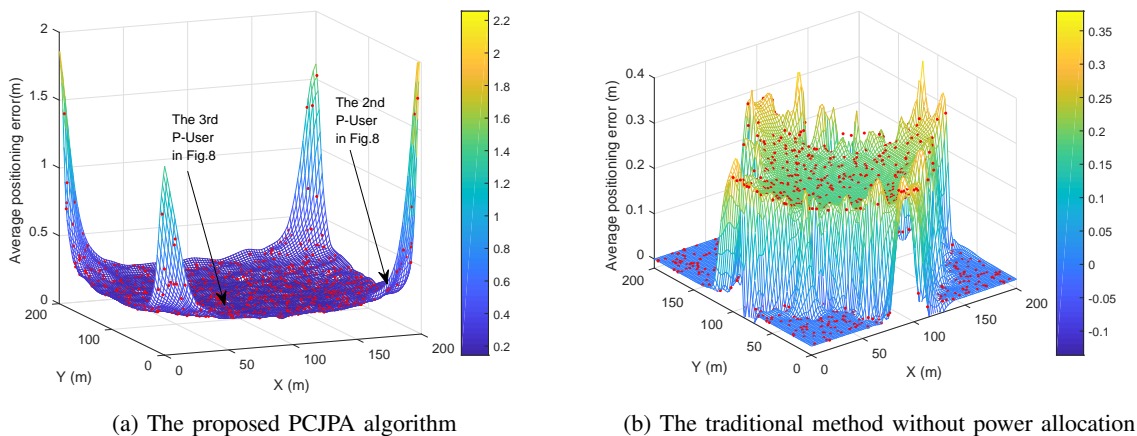


Fig. 5. The positioning signal's coverage and positioning accuracy ($B = 50\text{MHz}$, $P_{th} = 0.8\text{W}$, $\beta_{th} = 8 \times 10^{-3}$)

Fig. 5 shows the positioning signal's coverage and positioning accuracy of MS-NOMA signal by using the proposed PCJPA algorithm and the traditional equal-power transmission strategy, respectively. The positioning error is set to 0 if the P-User can not receive more than 3 gNBs which means there are no enough gNBs to position. From Fig. 5a, we can see all P-Users have positioning results which means the near-far effect is dramatically reduced. While from Fig.

5b, it is clear that a great amount of P-Users (50.8%) do not have positioning results by the traditional method as suffering severe near-far effect.

Detailed comparisons are presented in Table I. The positioning accuracy of MS-NOMA signal is much higher than the one of PRS. Specifically, the improvements of MS-NOMA signal (using the proposed PCJPA algorithm) are 93.7% and 93.1% compared to PRS with 20MHz and 50MHz bandwidth, respectively. Notice that the positioning error of PCJPA is a little higher than the equal-power strategy. This is because the edge of the coverage area have poor geometric distribution which lead to poor positioning accuracy, while these low accuracy P-Users are not averaged in the equal-power strategy as they have no positioning results. In fact, the positioning errors of the PCJPA algorithm are smaller than the ones of the equal-power strategy by examining the same area as Fig. 6 shows (0.17m v.s. 0.20m at 50MHz (15% improvement) and 0.41m v.s. 0.54m at 20MHz (24% improvement)). Only 10% P-Users' positioning errors by PCJPA algorithm are larger than the ones by equal-power strategy. While more than 50% P-Users do not have positioning results if power allocation is not executed. Therefore, the proposed PCJPA algorithm has excellent performances in both coverage and positioning accuracy than the traditional scheme.

TABLE I
THE COMPARISON BETWEEN DIFFERENT SIGNALS BY USING DIFFERENT POWER ALLOCATION STRATEGIES

Signal		MS-NOMA		PRS
Power allocation strategy		PCJPA	Equal power	Equal power
Positioning Error	20MHz	0.57m	0.54m	8.44m
	50MHz	0.21m	0.20m	3.17m

Fig. 7 illustrated the impact of different constraints and parameters on the positioning accuracy. From Fig. 7a, it is clear that the average positioning errors decrease with the increasing of the tolerable BER. Meanwhile, there is higher positioning accuracy with larger bandwidth. Notice that the curves tend to constant values when the tolerable BER increases. It is because the power budget limits the improvement of the performance. And it is clear that higher power budget can

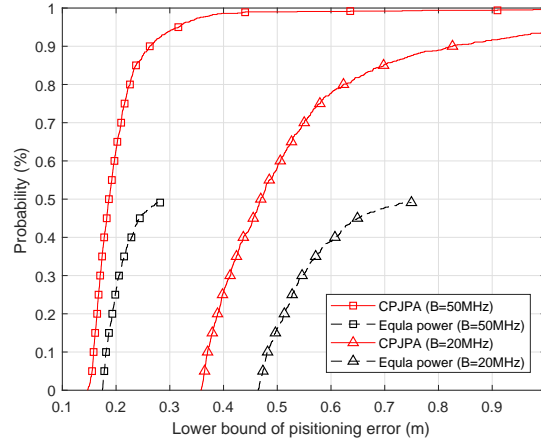
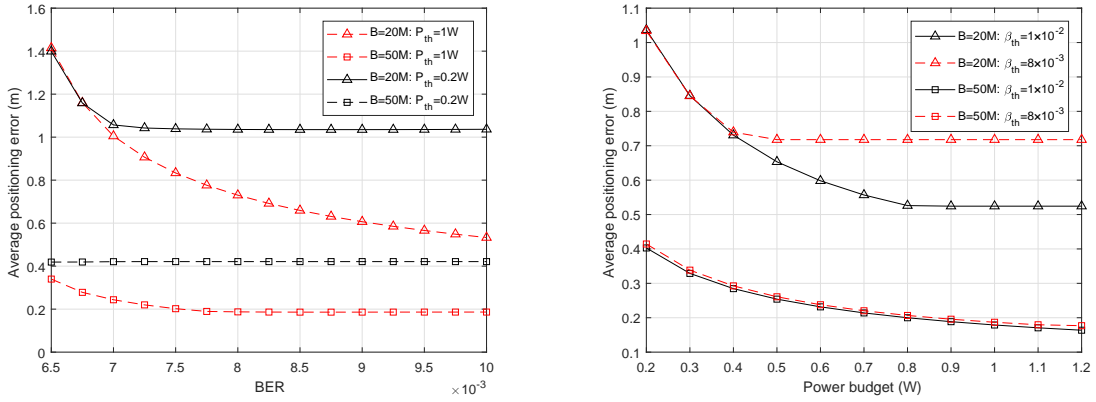


Fig. 6. The CDF of the MS-NOMA signal with different power allocation strategies ($P_{th} = 0.8W$, $\beta_{th} = 8 \times 10^{-3}$)

obtain a lower positioning error bound. On the other hand, the curve with a smaller bandwidth converges slowly. It is because the power of the positioning signal with a small bandwidth will be concentrated in a narrower range. Consequently, there will be more powers of P-Users leak to the neighbor C-Users as (3) and (4) show which leads to more interferences.

Fig. 7b shows that the average positioning error decreases with the increasing of the power budget. Similar to Fig. 7a, the curves tend to constant values when the power budget increases as well. This means the QoS constraint becomes dominant and the average positioning errors do not decrease although the total power increases. If we have a strict QoS constraint (smaller Ξ_{th}), the positioning error bound will be higher.

Fig. 8 illustrates the relationship between the allocated powers and the channel gains of the P-Users by examining one simulation. It shows that the worse channel states tend to allocate stronger positioning signals. This is exactly what we expected that the P-Users with worse channel states need stronger powers to obtain an accurate ranging. However, notice that there is a power disparity between the 2^{ed} and 3rd P-Users whose channel gains are similar. This is because the geometric-dilution λ in (1) also affects the positioning accuracy which is considered by the power allocation process. This can be observed in Fig. 5a as well: The location of the 2^{ed} P-User (coordinate: (178, 8)) is at the edge of the area compared to the center location of the 3rd P-User (coordinate: (79, 77)), so the former one has a stronger allocated power.



(a) Average positioning errors under different QoS requirements (b) Average positioning errors under different power budgets

Fig. 7. The impact of different constraints and parameters

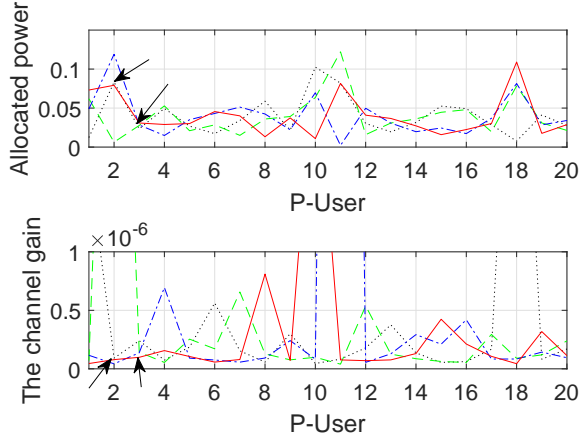


Fig. 8. The allocated powers with different channel gains (Different lines represent different gNBs) ($B = 50\text{MHz}$, $P_{th} = 0.8\text{W}$, $\beta_{th} = 8 \times 10^{-3}$)

VI. CONCLUSIONS

In this paper, we presented a feasibility study for a novel positioning-communication integrated signal called Multi-Scale Non-Orthogonal Multiple Access (MS-NOMA) for 5G positioning. The MS-NOMA signal superposes power configurable positioning signals on the communication ones to achieve high ranging accuracy and excellent signal coverage (less near-far effect). Like the normal NOMA signal, there are interferences between the communication and positioning signals. So, we analyzed the BER for communication and the ranging error for positioning when two

kinds of signals exist simultaneously. The results show the interaction is rather limited and the proposed MS-NOMA signal greatly improves the ranging accuracy than traditional 5G signal. In addition, because the positioning signals in the proposed MS-NOMA are power controllable and multiple accessible, we modeled a multi-user power allocation problem for an optimal positioning accuracy and signal coverage as a convex optimization problem under the QoS requirement and other constraints. Then, a novel Positioning-Communication Joint Power Allocation (PCJPA) algorithm was proposed for solving this problem. The numerical results show our proposed MS-NOMA signal with PCJPA algorithm improves the positioning accuracy and signal coverage dramatically than the traditional 5G signal with equal power transmission strategy.

APPENDIX

A. Derivation of the Horizontal Positioning Accuracy

Define $\varepsilon_\rho^m = [\varepsilon_\rho^{1m}, \varepsilon_\rho^{2m}, \dots, \varepsilon_\rho^{km}]^T$ as the ranging errors of P-User m , where ε_ρ^{km} represents the ranging error between gNB k and P-User m . Then, the positioning error of P-User m is [36]

$$\begin{aligned} \varepsilon_X^m &= \left[(G^m)^T G^m \right]^{-1} (G^m)^T \varepsilon_\rho^m \\ &= H^m \varepsilon_\rho^m \end{aligned} \quad (46)$$

where

$$G^m = \begin{bmatrix} l_x^{1m} & l_y^{1m} & l_z^{1m} \\ l_x^{2m} & l_y^{2m} & l_z^{2m} \\ \dots & \dots & \dots \\ l_x^{km} & l_y^{km} & l_z^{km} \end{bmatrix} \quad (47)$$

$$\begin{cases} l_x^{km} = (x_p^m - x_b^k) / \|X_b^k - X_p^m\| \\ l_y^{km} = (y_p^m - y_b^k) / \|X_b^k - X_p^m\| \\ l_z^{km} = (z_p^m - z_b^k) / \|X_b^k - X_p^m\| \end{cases} \quad (48)$$

where $X = [x, y, z]^T$ represents the coordinate. Subscript p and b represent P-User and gNB, respectively. Because the ranging errors from the gNBs are independent, their covariance matrix

is diagonal under the assumption that the range measuring is unbiased:

$$\begin{aligned}
(\sigma_\rho^m)^2 &= \text{cov}(\varepsilon_\rho^m, \varepsilon_\rho^m) \\
&= \begin{bmatrix} (\sigma_\rho^{1m})^2 & 0 & \dots & 0 \\ 0 & (\sigma_\rho^{2m})^2 & \dots & 0 \\ \dots & \dots & \dots & \dots \\ 0 & 0 & \dots & (\sigma_\rho^{km})^2 \end{bmatrix}
\end{aligned} \tag{49}$$

where $(\sigma_\rho^{km})^2 = \text{cov}(\varepsilon_\rho^{km}, \varepsilon_\rho^{km})$ represents the ranging error of the km^{th} positioning signal. Then, the covariance of the positioning error is

$$\begin{aligned}
(\sigma_X^m)^2 &= \text{cov}(\varepsilon_X^m, \varepsilon_X^m) \\
&= H^m (\sigma_\rho^m)^2 (H^m)^T
\end{aligned} \tag{50}$$

The diagonal elements represent the positioning accuracy of each direction. Then, the horizontal positioning accuracy can be expressed as

$$\Psi^m = \sqrt{\sum_{k \in \mathcal{K}} \left\{ \left[\sum_{i=1}^2 (\bar{h}_{ik}^m)^2 \right] (\sigma_\rho^{km})^2 \right\}} \tag{51}$$

where \bar{h}_{ik}^m s ($i \in \{1, 2, 3\}$) represent the elements of H^m . Note $\lambda^{km} = \sqrt{\sum_{i=1}^2 (\bar{h}_{ik}^m)^2}$ as the geometric-dilution, then we have (1).

B. Derivation of $(\sigma_\rho^{km})^2$

Note

$$A_0^m = \int_{B_0 - B_{fe}/2}^{B_0 + B_{fe}/2} f G_p^m(f + m\Delta f_p) \sin(\pi f D T_p) df \tag{52}$$

$$A_1^m = \int_{B_0 - B_{fe}/2}^{B_0 + B_{fe}/2} N_0 G_p^m(f + m\Delta f_p) \sin^2(\pi f D T_p) df \tag{53}$$

$$A_2^m = \int_{B_0 - B_{fe}/2}^{B_0 + B_{fe}/2} G_s^m(f + m\Delta f_p) G_p^m(f + m\Delta f_p) \sin^2(\pi f DT_p) df \quad (54)$$

$$A_3^m = \int_{B_0 - B_{fe}/2}^{B_0 + B_{fe}/2} G_q^{km}(f + m\Delta f_p) G_p^m(f + m\Delta f_p) \sin^2(\pi f DT_p) df \quad (55)$$

Then, (6) can be written as

$$(\sigma_\rho^{km})^2 = \frac{a(A_1^m + A_2^m + A_3^m)}{(2\pi)^2 |h_p^{km}|^2 P_p^{km} (A_0^m)^2} \quad (56)$$

Notice that there are multiple P-Users, i.e. the bandwidth of the positioning signal for one P-User is much smaller than the total bandwidth B . Moreover, the front-end bandwidth is larger than B as well. So we have $B_{fe} \gg 2/T_p$. Consequently, a DLL's narrow early-late spacing D can be applied³. When $D \rightarrow 0$, $\sin(\pi f DT_p)$ in (52)-(55) can be replaced by Taylor expansion around 0. Then, by taking (5), (7)-(8) into (52)-(55) and rearranging items, we have

$$A_0^m = \pi DT_p^2 \int_{-B_{fe}/2}^{B_{fe}/2} f^2 \text{sinc}^2(fT_p) df = \frac{1}{2\pi} DB_{fe} \quad (57)$$

$$A_1^m = \pi DT_p N_0 A_0^m \quad (58)$$

$$\begin{aligned} A_2^m &= D^2 T_p \sum_{k' \in \mathcal{K}} \sum_{n \in \mathcal{N}} |h_c^{m \leftarrow k'n}|^2 P_c T_c \int_{-B_{fe}/2}^{B_{fe}/2} \text{sinc}^2[(f + m\Delta f_p - n\Delta f_c) T_c] \sin^2(fT_p) df \\ &\stackrel{G \gg 1}{\approx} D^2 T_p T_c P_c \sum_{k' \in \mathcal{K}} \sum_{n \in \mathcal{N}} |h_c^{m \leftarrow k'n}|^2 \sin^2 \left[\pi \left(m - \frac{n}{G} \right) \right] \\ &\quad \times \int_{(Gm-n-1)\Delta f_c}^{(Gm-n+1)\Delta f_c} \text{sinc}^2[(f + m\Delta f_p - n\Delta f_c) T_c] df \\ &\approx D^2 T_p P_c \sum_{k' \in \mathcal{K}} \sum_{n \in \mathcal{N}} |h_c^{m \leftarrow k'n}|^2 \sin^2 \left(\frac{n}{G} \pi \right) \end{aligned} \quad (59)$$

³If B_{fe} is not large enough, the DLL correlation peak will be flattened which will deteriorate the performance of the phase discriminator.

$$A_3^m = \pi^2 D^2 T_p^4 \sum_{k' \in \mathcal{K}^k} |h_p^{k'm}|^2 P_p^{k'm} \underbrace{\int_{-B_{fe}/2}^{B_{fe}/2} f^2 \text{sinc}^4(fT_p) df}_{A_3} \quad (60)$$

where

$$\begin{aligned} \bar{A}_3 &\stackrel{B_{fe} \gg 2/T_p}{\approx} \int_{-\infty}^{\infty} \frac{\sin^4(\pi f T_p)}{\pi^4 f^2 T_p^4} df \\ &= \frac{1}{4\pi^4 T_p^4} \int_{-\infty}^{\infty} \left[\frac{4\sin^2(\pi f T_p)}{f^2} - \frac{\sin^2(2\pi f T_p)}{f^2} \right] df \\ &= \frac{1}{2\pi^2 T_p^3} \end{aligned} \quad (61)$$

Taking (57)-(61) back to (56) and rearranging items, we have

$$\begin{aligned} (\sigma_\rho^{km})^2 &\approx \frac{aT_p}{2} \left[\frac{N_0}{B_{fe} |h_p^{km}|^2 P_p^{km}} \right. \\ &\quad \left. + \frac{2P_c \sum_{k' \in \mathcal{K}} \sum_{n=1}^N |h_c^{m \leftarrow k'n}|^2 \sin^2\left(\frac{n}{G}\pi\right)}{B_{fe}^2 |h_p^{km}|^2 P_p^{km}} + \frac{\sum_{k' \in \mathcal{K}^k} |h_p^{k'm}|^2 P_p^{k'm}}{B_{fe}^2 |h_p^{km}|^2 P_p^{km}} \right] \\ &= \frac{aT_p^2}{2} \left(\frac{N_0}{B_{fe} T_p |h_p^{km}|^2 P_p^{km}} + \frac{BGP_c \sum_{k' \in \mathcal{K}} |h_c^{m \leftarrow k'}|^2}{B_{fe}^2 |h_p^{km}|^2 P_p^{km}} + \frac{\sum_{k' \in \mathcal{K}^k} |h_p^{k'm}|^2 P_p^{k'm}}{B_{fe}^2 T_p |h_p^{km}|^2 P_p^{km}} \right) \end{aligned} \quad (62)$$

where $|h_c^{m \leftarrow k'}|^2 = \frac{2}{N} \sum_{n \in \mathcal{N}} |h_c^{m \leftarrow k'n}|^2 \sin^2\left(\frac{n}{G}\pi\right)$ is defined as the normalized equivalent channel gain of the communication signal broadcast by gNB k' to the P-User m .

Let's define $(C/N_0)^{km} = |h_p^{km}|^2 P_p^{km} / N_0$ as the carrier-to-noise ratio of the km^{th} positioning signal, $(CPR)^{km \leftarrow k'} = \frac{2G |h_c^{m \leftarrow k'}|^2 P_c}{|h_p^{km}|^2 P_p^{km}}$ as the equivalent communication-to-positioning ratio of communication signal broadcast by gNB k' to positioning signal km , and $(PPR)^{km \leftarrow k'm} = \frac{|h_p^{k'm}|^2 P_p^{k'm}}{|h_p^{km}|^2 P_p^{km}}$ as the positioning-to-positioning ratio of the $k'm^{\text{th}}$ to the km^{th} positioning signal. Then we have (9).

C. Derivation of \tilde{P}_p^{km}

The KKT conditions of OP2 can be written as

$$\sum_{n \in \mathbb{N}_m} \tilde{\mu}^{kn} (I_{th}^{kn} - I^{kn}) = 0 \quad (63)$$

$$\tilde{\beta}^{km} \left(|h_p^{km}|^2 P_p^{km} - \varrho \Omega |h_p^{k'm}|^2 P_p^{k'm} \right) = 0 \quad (64)$$

$$\frac{\partial \tilde{\mathcal{L}} \left(\{P_p^{km}\}, \tilde{\mu}^{kn}, \tilde{\beta}^{km} \right)}{\partial P_p^{km}} = 0 \quad (65)$$

It is obvious that the optimal solution \tilde{P}_p^{km} satisfies (65). Thus, take (35) into (65), we have

$$\begin{aligned} \frac{\partial \tilde{\mathcal{L}}}{\partial P_p^{km}} &= \frac{-\frac{1}{M} \partial (\lambda^{km} \sigma_\rho^{km})^2 - \nu^k P_p^{km}}{\partial P_p^{km}} + \frac{\partial \sum_{n \in \mathbb{N}_m} \tilde{\mu}^{kn} (I_{th}^{kn} - I^{kn})}{\partial P_p^{km}} \\ &\quad + \frac{\partial \left\{ \tilde{\beta}^{km} \left(|h_p^{km}|^2 P_p^{km} - \varrho \Omega |h_p^{k'm}|^2 P_p^{k'm} \right) \right\}}{\partial P_p^{km}} \\ &= -\frac{1}{M} \left(\frac{\lambda^{km} \tilde{\sigma}_\rho^{km}}{P_p^{km}} \right)^2 - \nu^k - \sum_{n \in \mathbb{N}_m} \tilde{\mu}^{kn} \underbrace{\frac{\partial I^{kn}}{\partial P_p^{km}}}_{J^{kn \leftarrow m}} + \tilde{\beta}^{km} |h_p^{km}|^2 \end{aligned} \quad (66)$$

By taking (3) into (66), we have

$$J^{kn \leftarrow m} = \sum_{k' \in \mathcal{K}} \left| h_p^{kn \leftarrow k'm} \right|^2 T_p \text{sinc}^2 \left(m - \frac{n}{G} \right) \quad (67)$$

Then, by setting (66) to 0, we can obtain the optimal power allocation solution as (40) shows.

D. Subgradient Method of the Lagrange Dual Function

For a set of dual variable $\{\tilde{\mu}, \tilde{\nu}, \tilde{\beta}\}$, it is known that if $g^k(\tilde{\mu}^{kn}) \geq g^k(\mu^{kn}) + s(\tilde{\mu}^{kn} - \mu^{kn})$ holds for any feasible $\tilde{\mu}^{kn}$, then s must be the subgradient of $g^k(\mu^{kn})$ at μ^{kn} . Then the Lagrange

dual function of sub-problem (29) is

$$\begin{aligned}
g^k(\tilde{\mu}, \tilde{\nu}, \tilde{\beta}) &= \max_{P_p^{km}} \mathcal{L}(\{P_p^{km}\}, \tilde{\mu}, \tilde{\nu}, \tilde{\beta}) \\
&= \max_{P_p^{km}} \left[-\frac{1}{M} \sum_{m \in \mathcal{M}} \lambda^{km} (\tilde{\sigma}_\rho^{km})^2 + \sum_{n \in \mathcal{N}} \tilde{\mu}^{kn} (I_{th}^{kn} - I^{kn}) \right. \\
&\quad \left. + \tilde{\nu}^k \left(P_{th}^k - \sum_{m \in \mathcal{M}} P_p^{km} \right) + \sum_{m \in \mathcal{M}} \tilde{\beta}^{km} \left(|h_p^{km}|^2 P_p^{km} - \varrho \Omega |h_p^{k'm}|^2 P_p^{k'm} \right) \right] \\
&\geq -\frac{1}{M} \sum_{m \in \mathcal{M}} \lambda^{km} (\tilde{\sigma}_\rho^{km})^2 + \sum_{n \in \mathcal{N}} \tilde{\mu}^{kn} (I_{th}^{kn} - I^{kn}) \\
&\quad + \tilde{\nu}^k \left(P_{th}^k - \sum_{m \in \mathcal{M}} P_p^{km} \right) + \sum_{m \in \mathcal{M}} \tilde{\beta}^{km} \left(|h_p^{km}|^2 P_p^{km} - \varrho \Omega |h_p^{k'm}|^2 P_p^{k'm} \right) \\
&= g^k(\mu, \nu, \beta) + (\tilde{\nu}^k - \nu^k) \left(P_{th}^k - \sum_{m \in \mathcal{M}} P_p^{km} \right) + \sum_{n \in \mathcal{N}} (\tilde{\mu}^{kn} - \mu^{kn}) (I_{th}^{kn} - I^{kn}) \\
&\quad + \sum_{m \in \mathcal{M}} (\tilde{\beta}^{km} - \beta^{km}) \left(|h_p^{km}|^2 P_p^{km} - \varrho \Omega |h_p^{k'm}|^2 P_p^{k'm} \right) \tag{68}
\end{aligned}$$

REFERENCES

- [1] J. A. del Peral-Rosado, R. Raulefs, J. A. Lopez-Salcedo, and G. Seco-Granados, "Survey of cellular mobile radio localization methods: from 1G to 5G," *IEEE Communications Surveys and Tutorials*, vol. PP, no. 99, pp. 1–1, 2018.
- [2] M. Shojafar, N. Cordeschi, and E. Baccarelli, "Energy-efficient adaptive resource management for real-time vehicular cloud services," *IEEE Transactions on Cloud Computing*, vol. PP, no. 99, pp. 1–1, 2016.
- [3] H. Liang, G. X. Gao, T. Walter, and P. Enge, "Automated verification of potential GPS signal-in-space anomalies using ground observation data," in *Position Location and Navigation Symposium*, 2012.
- [4] L. Deng and S. Ye, "Vehicle information system design based on Beidou navigation satellite system," in *IEEE International Conference on Information and Automation*, Aug 2015, pp. 867–870.
- [5] L. Yin, Q. Ni, and Z. Deng, "A GNSS/5G integrated positioning methodology in D2D communication networks," *IEEE Journal on Selected Areas in Communications*, vol. 36, no. 2, pp. 351–362, 2018.
- [6] J. Jeon, Y. Kong, Y. Nam, and K. Yim, "An indoor positioning system using Bluetooth RSSI with an accelerometer and a barometer on a smartphone," in *International Conference on Broadband and Wireless Computing, Communication and Applications*, 2016, pp. 528–531.
- [7] S. Tomic, M. Beko, and D. Rui, "RSS-based localization in wireless sensor networks using convex relaxation: Noncooperative and cooperative schemes," *IEEE Transactions on Vehicular Technology*, vol. 64, no. 5, pp. 2037–2050, 2014.
- [8] L. Yin, Q. Ni, and Z. Deng, "Intelligent multisensor cooperative localization under cooperative redundancy validation," *IEEE Transactions on Cybernetics*, pp. 1–13, 2019.

- [9] H. Zou, M. Jin, H. Jiang, L. Xie, and C. J. Spanos, "WinIPS: WiFi-based non-intrusive indoor positioning system with online radio map construction and adaptation," *IEEE Transactions on Wireless Communications*, vol. 16, no. 12, pp. 8118–8130, Dec 2017.
- [10] H. Shuai, Z. Gong, W. Meng, L. Cheng, D. Zhang, and W. Tang, "Automatic precision control positioning for wireless sensor network," *IEEE Sensors Journal*, vol. 16, no. 7, pp. 2140–2150, 2016.
- [11] J. Chen, X. Ge, and Q. Ni, "Coverage and handoff analysis of 5G fractal small cell networks," *IEEE Transactions on Wireless Communications*, vol. 18, no. 2, pp. 1263–1276, Feb 2019.
- [12] Y. Zhou, V. W. S. Wong, and R. Schober, "Coverage and rate analysis of millimeter wave NOMA networks with beam misalignment," *IEEE Transactions on Wireless Communications*, vol. 17, no. 12, pp. 1–1, 2018.
- [13] R. M. Vaghefi and R. M. Buehrer, "Cooperative UTDOA positioning in LTE cellular systems," in *Globecom Workshops*, 2016.
- [14] X. Cui, A. Gulliver, H. Song, and J. Li, "Real-time positioning based on millimeter wave device to device communications," *IEEE Access*, vol. 4, no. 99, pp. 5520–5530, 2017.
- [15] 3GPPTR38.855v.16.0.0, "Study on NR positioning support," 2019.
- [16] J. Schloemann, H. S. Dhillon, and R. M. Buehrer, "A tractable analysis of the improvement in unique localizability through collaboration," *IEEE Transactions on Wireless Communications*, vol. 15, no. 6, pp. 3934–3948, 2015.
- [17] Z. Deng, Y. U. Yanpei, Y. Xie, and N. Wan, "Situation and development tendency of indoor positioning," *China Communications*, vol. 10, no. 3, pp. 42–55, 2013.
- [18] T. Manna and A. Kole, "Performance analysis of secure DSSS multiuser detection under near-far environment," in *International Conference on Intelligent Control Power and Instrumentation*, 2016.
- [19] J. Schloemann, H. S. Dhillon, and R. M. Buehrer, "A tractable metric for evaluating base station geometries in cellular network localization," *IEEE Wireless Communications Letters*, vol. 5, no. 2, pp. 140–143, 2015.
- [20] C. H. Chen and K. T. Feng, "Enhanced distance and location estimation for broadband wireless networks," *IEEE Transactions on Mobile Computing*, vol. 14, no. 11, pp. 1–1, 2015.
- [21] W. Yu, L. Musavian, and Q. Ni, "Link-layer capacity of NOMA under statistical delay QoS guarantees," *IEEE Transactions on Communications*, vol. 66, no. 10, pp. 4907–4922, Oct 2018.
- [22] Y. Liu, Z. Qin, M. ElKashlan, Z. Ding, A. Nallanathan, and L. Hanzo, "Nonorthogonal multiple access for 5G and beyond," *Proceedings of the IEEE*, vol. 105, no. 12, pp. 2347–2381, 2017.
- [23] L. Yin, J. Cao, K. Lin, Z. Deng, and Q. Ni, "A novel positioning-communication integrated signal in wireless communication systems," *IEEE Wireless Communications Letters*, pp. 1–1, 2019.
- [24] A. K. Karmokar, M. Naem, and A. Anpalagan, "Energy-efficient subcarrier power allocation for cognitive radio networks using statistical interference model," in *IEEE International Symposium on Personal, Indoor, and Mobile Radio Communications*, 2015.
- [25] N. Forouzan and S. A. Ghorashi, "New algorithm for joint subchannel and power allocation in multi-cell OFDMA-based cognitive radio networks," *IET Communications*, vol. 8, no. 4, pp. 508–515, March 2014.
- [26] X. Ding and Q. Li, "Joint power control and time allocation for wireless powered underlay cognitive radio networks," *IEEE Wireless Communications Letters*, vol. PP, no. 99, pp. 1–1, 2017.
- [27] C. Yan, A. Bayesteh, Y. Wu, B. Ren, S. Kang, S. Sun, X. Qi, Q. Chen, B. Yu, and Z. Ding, "Toward the standardization of

- non-orthogonal multiple access for next generation wireless networks,” *IEEE Communications Magazine*, vol. 56, no. 3, pp. 19–27, 2018.
- [28] J. Zhao, Y. Liu, K. K. Chai, A. Nallanathan, Y. Chen, and Z. Han, “Spectrum allocation and power control for non-orthogonal multiple access in HetNets,” *IEEE Transactions on Wireless Communications*, vol. 16, no. 9, pp. 5825–5837, Sep. 2017.
- [29] E. J. Zhong and T. Z. Huang, “Geometric dilution of precision in navigation computation,” in *International Conference on Machine Learning and Cybernetics*, 2009.
- [30] Y. Liu, Z. Ding, M. ElKashlan, and H. V. Poor, “Cooperative non-orthogonal multiple access with simultaneous wireless information and power transfer,” *IEEE Journal on Selected Areas in Communications*, vol. 34, no. 4, pp. 938–953, 2016.
- [31] J. W. Betz and K. R. Kolodziejcki, “Generalized theory of code tracking with an early-late discriminator Part I: Lower bound and coherent processing,” *IEEE Transactions on Aerospace and Electronic Systems*, vol. 45, no. 4, pp. 1538–1556, 2009.
- [32] Boyd, Vandenberghe, and Foybusovich, *Convex Optimization*, 2004.
- [33] R. Zhang, “Optimal power control over fading cognitive radio channel by exploiting primary user CSI,” in *IEEE Global Communications Conference (GLOBECOM)*, Nov 2008, pp. 1–5.
- [34] L. Li and C. Xu, “On ergodic sum capacity of fading channels in OFDMA-based cognitive radio networks,” *IEEE Transactions on Vehicular Technology*, vol. 63, no. 9, pp. 4334–4343, Nov 2014.
- [35] J. A. del Peral-Rosado, J. A. Lopez-Salcedo, G. Seco-Granados, F. Zanier, and M. Crisci, “Joint channel and time delay estimation for LTE positioning reference signals,” in *ESA Workshop on Satellite Navigation Technologies European Workshop on GNSS Signals and Signal Processing*, Dec 2012, pp. 1–8.
- [36] Y. Lu, Z. Deng, Z. Di, and E. Hu, “Quality assessment method of GNSS signals base on multivariate dilution of precision,” in *European Navigation Conference*, 2016.